Research Square

Preprints are preliminary reports that have not undergone peer review.
They should not be considered conclusive, used to inform clinical practice,
or referenced by the media as validated information.

In Vitro Anti-Tubercular Evaluation and Selective Fe^{3+} Fluorescence Turn-Off Sensing of Aspartic Acid-Catalyzed Tetraketone and Xanthene Derivatives in Aqueous Medium

Asif Shariff A.
University of Madras
Mohan Ram E.
University of Madras
Abdul Bazith M. I.
University of Madras
Raees Ahmed A. K.
University of Madras
Azger Dusthackeer V. N.
National Institute of Research in Tuberculosis
Ambrose Rajkumar M.
Sivakumar Sivalingam
Vel Tech Rangarajan Dr. Sagunthala R&D Institute of Science and Technology
Thajudeen Habeebullah
University of Madras
Jamal Ahamed V. S.
jamalahamed@thenewcollege.edu.in

University of Madras

Research Article

Keywords:

Posted Date: August 3rd, 2026

DOI: https://doi.org/10.21203/rs.3.rs-10270755/v1

License: This work is licensed under a Creative Commons Attribution 4.0 International License.
Read Full License

Additional Declarations: No competing interests reported.

In Vitro Anti-Tubercular Evaluation and Selective Fe^{3+} Fluorescence Turn-Off Sensing of Aspartic Acid-Catalyzed Tetraketone and Xanthene Derivatives in Aqueous Medium

A. Asif Shariff[a], E. Mohan Ram[a], M. I. Abdul Bazith[a], A. K. Raees Ahmed[a], V. N. Azger Dusthackeer[b], M. Ambrose Rajkumar[d], Sivakumar Sivalingam[c]*, Habeebullah Thajudeen[a]*, V. S. Jamal Ahamed[a]*

[a] PG & Research Department of Chemistry, The New College (Autonomous), Chennai-600 014, Tamil Nadu India

[b]National Institute for Research in Tuberculosis, Chennai-600 031, Tamilnadu, India

[c]Department of Chemistry, Vel Tech Rangarajan Dr.Sagunthala R&D Institute of Science and Technology, Avadi, Chennai-600 062, Tamil Nadu, India

[d]Department of Physics, Kristu Jayanti Deemed to be University, Bengaluru.

* Correspondence: jamalahamed@thenewcollege.edu.in

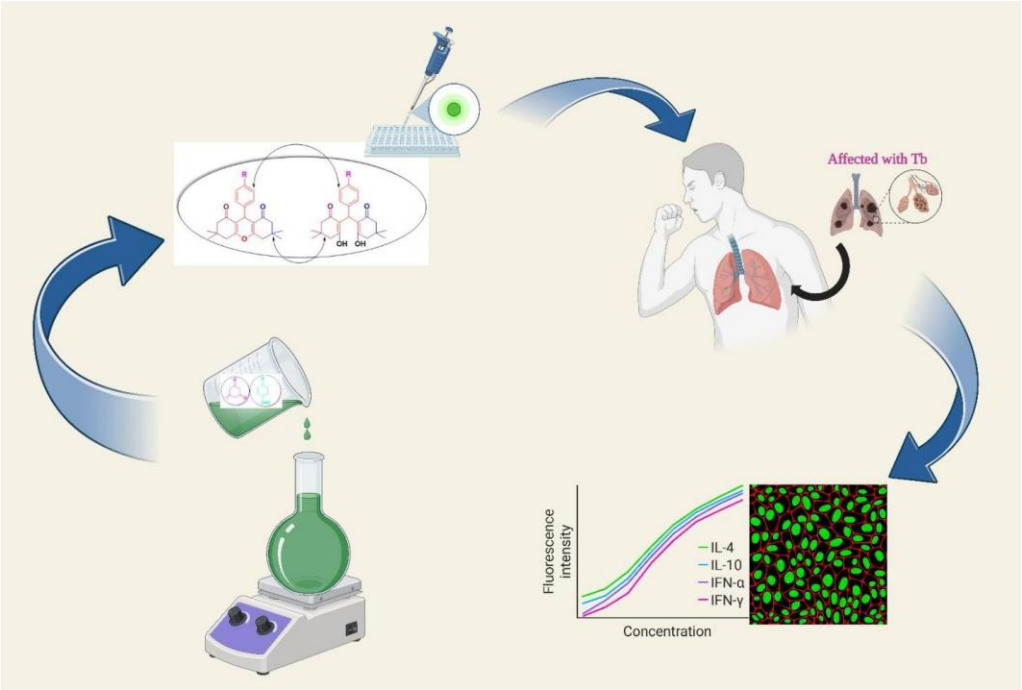
thajudeen@thenewcollege.edu.in

drsivakumars@veltech.edu.in

Abstract

Tuberculosis (TB) is a major global health issue, and the rise of drug-resistant strains makes it even more challenging to treat. Here, we report the design and synthesis of tetraketone products **(3a–3l)** and their cyclised xanthene derivatives **(4a–4i)**, via an aspartic acid-mediated reaction in water, and evaluate their *in vitro* activity against *Mycobacterium tuberculosis* H37Rv. The most active compounds were **3k** and **3l**, which each exhibited a minimum inhibitory concentration (MIC) of 31.25 μg/mL, and a number of other tetraketone derivatives also displayed moderate activity. The xanthene series were less active, with MICs of 125 μg/mL or higher, suggesting that the tetraketone motif is the more relevant pharmacophore in the development of anti-TB drugs. Aside from their biological activity, compounds **3a–3l** were also tested for their fluorescent sensing properties towards a series of inorganic cations (K^+, Ca^{2+}, Mn^{2+}, Co^{2+}, Ni^{2+}, Cu^{2+}, Zn^{2+}, Fe^{3+}, Hg^{2+}, Sn^{2+}, Cd^{2+} and Al^{3+}) using fluorescence spectroscopy (λ_{ex} = 350 nm, emission 400–550 nm). Fe^{3+} in particular induced a significant decrease in emission at 414 nm for compound **3b**, with no change in the emission profile for the remaining cations. This turn-off response is attributed to Fe^{3+} binding at the chelating sites of **3b**, which is rich in hydroxyl groups, and subsequent non-radiative decay

via a chelation-enhanced quenching (CHEQ) mechanism. Overall, these findings show that the tetraketone core is a promising scaffold for the development of both anti-TB drugs and Fe^{3+}-selective fluorescent sensors.



Introduction

In natural products, tetraketones are derived from 1,3-dicarbonyl compounds, which are associated with a wide range of biological activities. Among them, cyclohexane-1,3-dione is one of the most important molecules, first described by Merling in 1894. Tetraketones or 2,2'-Arylmethylene bis(3-hydroxy-5,5-dimethyl-2-cyclohexene-1-one) and its analogues are oxygen-containing heterocycles that function as important intermediates in the field of pharmaceutical chemistry. Based on this core structure, several related compounds have also been synthesized and documented in the literature. These compounds have demonstrated notable pharmacological potential, exhibiting a wide range of biological activities such as antioxidant, antidepressant[1], and antimalarial effects. In addition, they have been reported to inhibit key enzymes including lipoxygenase[2] and tyrosinase[3], and have also found

applications in laser-based technologies.[4–14] Moreover, tetraketones are widely regarded as versatile precursors or building blocks for the synthesis of valuable compounds such as xanthenes, thioxanthenes, and acridines. As well, xanthene, specifically 1,8-dioxo-octahydroxanthene derivatives, exhibit several biological activities.

Xanthene-derived scaffolds are frequently incorporated into biologically active compounds, underscoring their importance in the fields of drug discovery and therapeutic innovation. Owing to their diverse pharmacological profiles, xanthene derivatives have gained substantial attention among medicinal chemists. These molecules are known to possess a wide spectrum of biological activities, such as antibacterial,[15] antidepressant, antiviral,[16] anticancer, antiplasmodial, and anti-inflammatory properties.[17–21] In addition to their pharmacological relevance, xanthene scaffolds have found important applications in materials science, such as fluorescent sensing, pH-responsive materials, agrochemicals, corrosion inhibitors, and photodynamic therapy for tumor cell destruction. [22–27]

Although tetraketones and xanthenes have been widely reported to exhibit diverse biological activities, their potential against Tuberculosis remains relatively underexplored, particularly in studies involving *Mycobacterium tuberculosis*. As the etiological agent of Tuberculosis, *M. tuberculosis* remains the foremost cause of mortality from a single infectious pathogen and continues to pose a significant global health challenge, accounting for approximately 10.5 million new infections and over 1.6 million deaths in 2021.[28] It is primarily a pulmonary infection with symptoms such as chest pain, coughing, fever, fatigue and weight loss. A common challenge in treating tuberculosis is its non-replicating persistent state, which makes conventional drug treatments less effective. Poor treatment adherence, long treatment duration, improper chemotherapy management, and socio-economic factors are contributing to the rise in drug-resistant tuberculosis (DRTB), including MDR-TB, XDR-

TB, and TDR-TB. This results in a continuous need to develop alternative TB treatments that can effectively combat drug-resistant strains of *Mycobacterium tuberculosis*.[29]

In recent years, a wide range of anti-tuberculosis agents originating from both natural sources and synthetic strategies have been reported; however, there remains a pressing need to develop new anti-TB compounds featuring innovative chemical scaffolds. Consequently, tetraketone and xanthene derivatives have attracted substantial attention and have been investigated extensively for their biological potential. Despite these encouraging findings, certain challenges and inconsistencies persist, particularly in relation to their synthetic methodologies. Even so, a few synthetic processes have been developed using various catalytic systems such as $(Et)_4NOH$,[30][BCMIM]Cl)],[31]NaOH,[32]KOH,[33]piperidine,[34] proline[35], cetyltrimethylammonium bromide (CTMAB), [36][H-Pyrr][HSO4],[37] L-histidine in ionic liquid,[38]nanoSiO_2Cl,[39]amino-appended□-cyclodextrin,[40]Fe-zeolite,[41] 2-aminopyrazine,[42]sodiumalginate,[43]piperazine–GO,[44]SO_3H-functionalized nano-MGO-D-NH_2,[45]Cs-EDTA-Cell network,[46]nano-α-Al_2O_3 supported ammoniumdihydrogen phosphate ($NH_4H_2PO_4/Al_2O_3$),[47] proline- or propylamine-modified SBA-15, [48] PMO-ICS [49], and $FeNi_3$–SiO_2 nanoparticles.[50] However, there is still a need for more efficient and environmentally friendly methods to improve these synthetic approaches.

Modern organic synthesis, therefore, demands alternative strategies that can reduce waste and avoid harmful reagents commonly used in traditional procedures. For this reason, green chemistry is receiving a great deal of attention. Current research is mainly focused on the use of eco-friendly methodologies, non-hazardous and non-toxic chemicals, green catalysts, and green solvents. In particular, the use of solvents is a major concern because they often contribute to hazards, toxicity, pollution, and waste treatment difficulties. Moreover, solvents usually account for the largest portion of wasted mass in many synthetic

processes. Therefore, finding safer and more sustainable alternatives to conventional organic solvents has become an important goal in modern green chemistry.

In this context, the use of water as a solvent for organic reactions has attracted great interest [51–53] among chemists over the past few decades, sometimes leading to surprising and unexpected outcomes. Considerable progress has been achieved in carrying out organic reactions in water or aqueous media, and many new transformations can now be performed efficiently under such environmentally friendly conditions.

Amino acids have gained significant attention as organocatalysts in asymmetric synthesis owing to their non-toxic character, renewable origin, and economic affordability. [22] For instance, proline is extensively used as an organocatalysts in aldol condensation and Ullmann reactions, whereas tryptophan and alanine are employed in asymmetric Mannich reactions. In 2018, we explored the use of amino acids as catalyst to synthesize Dihydroquinazolinones in water, and found that aspartic acid is the most efficient.[54]

Adopting environmentally friendly and sustainable methodologies is therefore strongly encouraged. As part of our work on synthesis of natural products and developing sustainable methodologies, we investigated developing a greener way to synthesize tetraketones using readily available substrates. Here, we present a one-pot synthesis of tetraketones and xanthene derivatives using readily available commercial aldehydes catalyzed by aspartic acid in water.

RESULTS AND DISCUSSION:

Our current work explores bio-based organocatalysts for carbonyl transformations, and we were particularly interested in evaluating amino acids as environmentally benign catalysts for the present reaction.[22] In the previous study,[54] aspartic acid

demonstrated excellent catalytic activity under mild aqueous conditions in the synthesis of 2,3-dihydroquinazolin-4(1H)-one derivatives. In light of these findings, we examined whether it can be applied in the current transformation. For determining the catalyst loading of aspartic acid at 10 mol%, a preliminary study was conducted. The reaction yielded only 34.8%, which was elevated to 55.4% at 20 mol% and optimal efficiency was achieved at 30 mol%, resulting in 85% yield for the desired product. Further increasing to 40 mol% did not result in additional improvement (65.8%), indicating that 30 mol% is sufficient for effective catalysis.

Table 1: The effect of mol% of aspartic acid on the optimization reactions

Trial	mol% of Aspartic acid	Yield (%)*
1	5	21.2
2	10	34.8
3	15	42.5
4	20	55.4
5	25	69.1
6	**30**	**85.0**
7	35	73.8
8	40	65.8

*Reaction conditions: H_2O (5 mL), Room temp., 24 h.

Based on this optimization, a 30 mol% catalyst loading was chosen to screen various amino acids under identical conditions. Specifically, glycine and tryptophan exhibited lower catalytic activity, while proline, histidine, and serine yielded moderate results, and glutamic acid had improved performance (79.9%), whereas aspartic acid upheld superior, delivering the highest yield (85%). Table 2 It is important to note that no products were formed without a catalyst, confirming the role of the amino acid. Owing to its bifunctional nature, aspartic acid can activate carbonyl substrates through acid-assisted enolization pathways. Its two carboxylic

acid groups are capable of acting as activating sites via hydrogen bonding and Brønsted acid catalysis.

Table 2: Screening of amino acid catalysts for the synthesis of tetraketone derivative **3a**

Entry	Catalyst	Catalyst (mol%)	Time (hr)	Yield (%)
1	Glycine	30	24	57.2
2	Proline	30	24	69.4
3	Tryptophan	30	24	43.6
4	Histidine	30	24	70.6
5	Serine	30	24	71.4
6	Glutamic acid	30	24	79.9
7	**Aspartic acid**	**30**	**24**	**85.0**
8	No Catalyst	**-**	24	Trace

Following identification of aspartic acid (30 mol%) as the optimal catalyst, the effect of reaction temperature and time on reaction yield was systematically investigated in water, and initially the reaction was conducted at 80 °C. After 5 h, the yield reached 58.6%, gradually increasing to 65.8% after 10 h, reaching 85% after 24 h at room temperature of prolonged reaction time. Table 3

Table 3: Optimization (variation of temperature and time) experiments by using aspartic acid catalyst (30 mol %).

Entry	Solvent	Temperature	Time (hr)	Yield (%)
1	H_2O	80^0 C	5	58.6
2	H_2O	80^0 C	10	65.8
3	H_2O	80^0 C	24	73.5

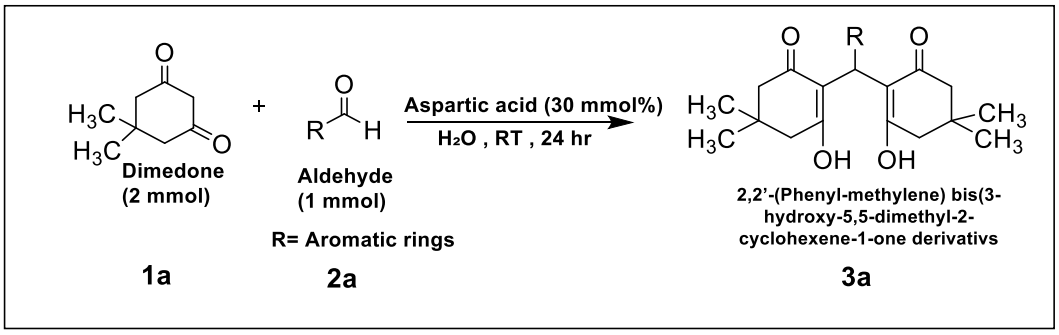
4	H_2O	R.T	5	72.4
5	H_2O	R.T	10	76.1
6	**H_2O**	**R.T**	**24**	**85**

According to these findings, the transformation occurs more efficiently under ambient conditions, indicating that higher temperatures are not conducive to the catalytic pathway. These non-covalent interactions may be partially disrupted at elevated temperatures due to enhanced hydrogen-bonding interactions and better stabilization of key intermediates in aqueous medium.

Next, using the optimized conditions, we explored the substrate scope by reacting functionalized aromatic aldehydes with dimedone to obtain tetraketone and xanthene derivatives through condensation in the presence of aspartic acid (30 mol%). A mixture of aromatic aldehyde 1 (1.0 equiv) and dimedone 2 (2.0 equiv) was stirred at room temperature in water using aspartic acid as catalyst.

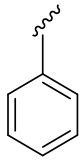
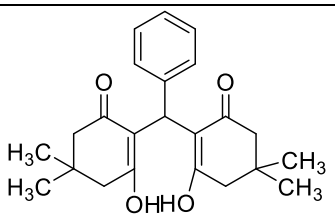
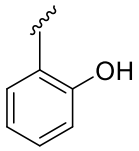
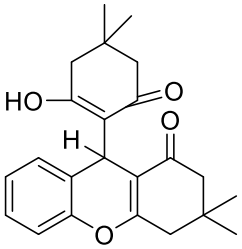
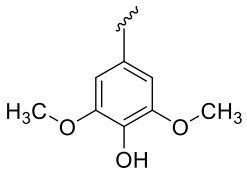
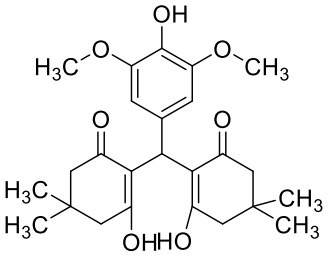
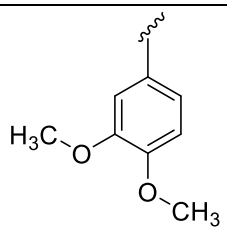
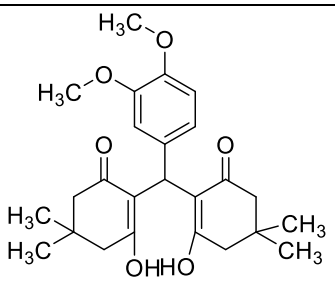
The developed protocol exhibited broad generality, accommodating a diverse array of structurally distinct aldehydes. Variations in the electronic nature of the aryl substituents had minimal impact on the efficiency of the condensation reaction. Under the optimized reaction conditions, a wide range of aldehydes including aromatic, heteroaromatic, and sterically demanding substrates bearing either electron-donating or electron-withdrawing substituents were found to be well tolerated.

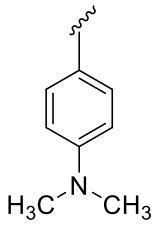
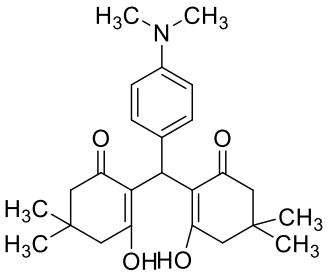
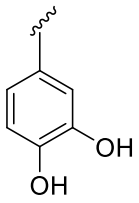
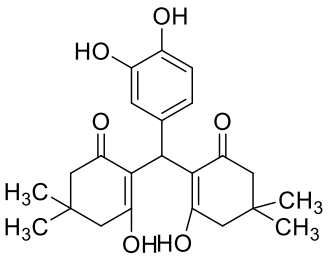
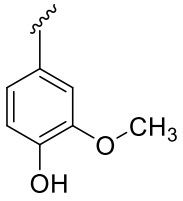
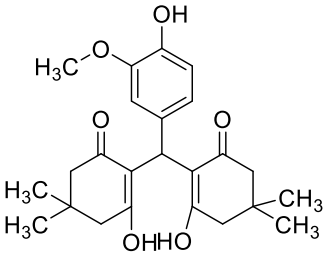
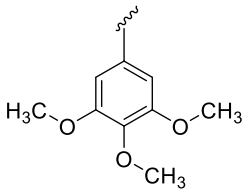
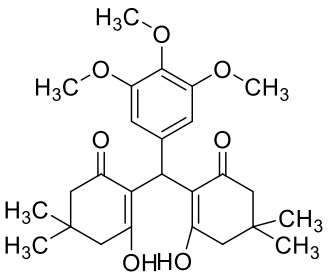
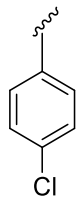
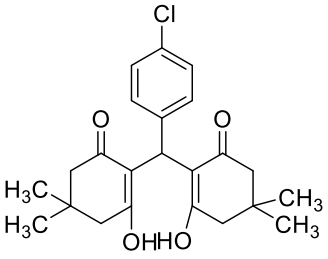
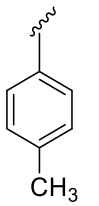
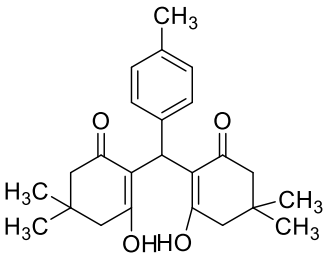
The investigation was further expanded by reacting dimedone 1a (2.0 equiv) with various aromatic aldehydes 2a (1.0 equiv) in the presence of aspartic acid as a catalyst under identical conditions, in order to assess how the catalyst affects the distribution of products. In Table 4, we present some examples. The transformation was clean and efficient, yielding good to excellent yields of substituted tetraketone derivatives **(3a – 3l)**. All the structures of tetraketone and xanthene derivatives were characterized via ^{1}H and ^{13}C NMR spectroscopy and by HRMS data.

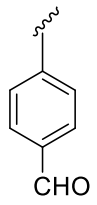
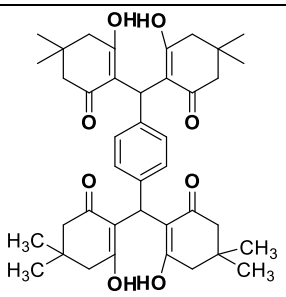
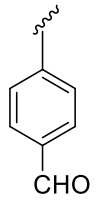
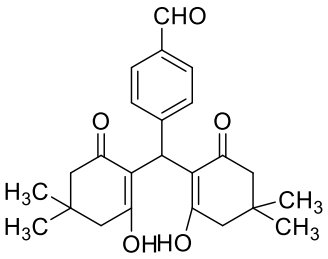


Scheme 1: Green synthesis of tetraketones by aspartic acid catalyst in H_2O medium.

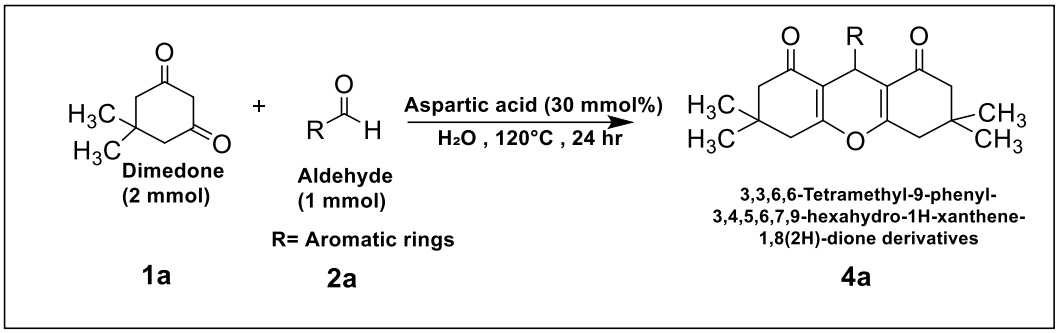
Table 4: Knoevenagel reaction of various aldehydes using by aspartic acid catalyst in H_2O medium.

Entry	R	PRODUCT	TIME-RT	YIELD
3a			24	95
3b			24	79
3c			24	80
3d			24	86

3e			24	81
3f			24	87
3g			24	77
3h			24	74
3i			24	82
3j			24	83

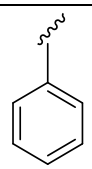
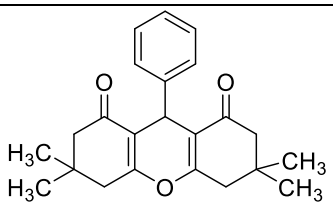
3k			24	82
3l			24	84

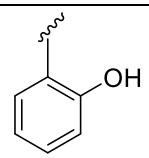
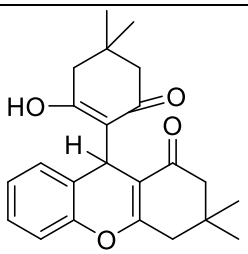
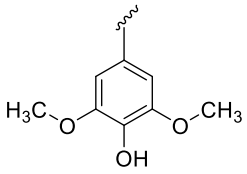
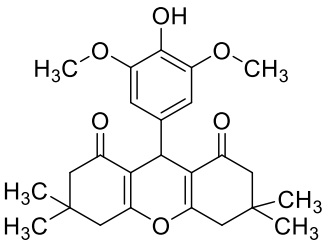
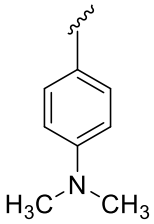
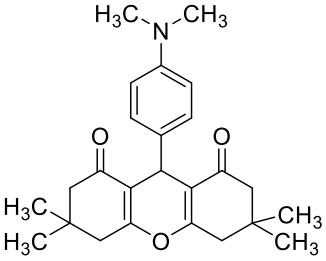
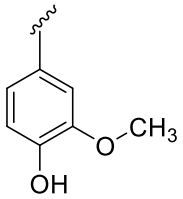
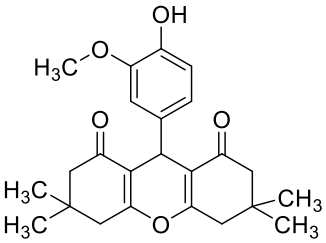
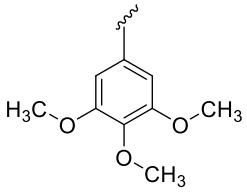
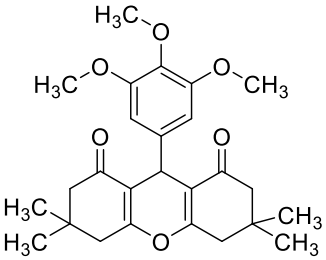
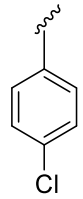
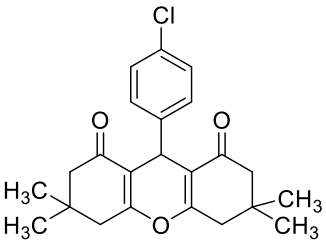
*All reactions were carried out with aromatic aldehyde (2 mmol), dimedone (4 mmol), aspartic acid (30% mol) and H_2O (10 mL) under room temperature conditions. In entries 3k, (8 mmol) of dimedone and aromatic aldehyde (2 mmol) was used.

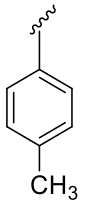
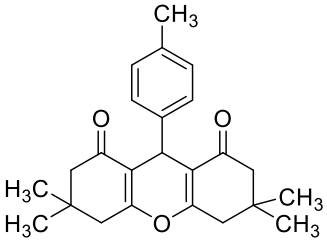
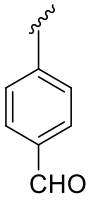
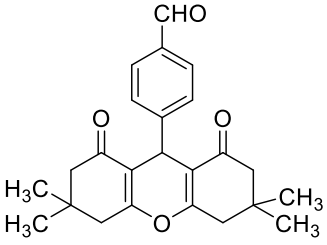


Scheme 2: Green synthesis of xanthene by aspartic acid catalyst in H_2O medium.

Table 5: Knoevenagel reaction of various aldehydes using by aspartic acid catalyst in H_2O medium.

Entry	**R**	**PRODUCT**	**TIME-120°C**	**YIELD**
4a			24	85

4b			24	79
4c			24	81
4d			24	84
4e			24	71
4f			24	79
4g			24	79

4h			24	75
4i			24	80

*All reactions were carried out with aromatic aldehyde (2 mmol), dimedone (4 mmol), aspartic acid (30% mol) and H_2O (10 mL) under reflux conditions at 120°C.

The structure of compound 3a could be easily identified by the appearance of characterized methine proton peak at δ 5.54 ppm and the signals at δ 2.48 and 1.23 ppm, correspond to the methylene and methyl groups. All the aromatic protons of 3a were in the range of δ 7.28–7.08 ppm. Also, compound 3a showed one signal at δ 11.90 ppm. Evaluation of ^{13}C NMR of compound 3a revealed that the characteristic peak of carbonyl compound is at δ 138.09 ppm. All the aromatic and aliphatic carbons of the synthesized compounds were in the range of 138.09–27.44 ppm. The HRMS spectra of the designed hybrids exhibited characteristic $[M+H]^+$ peaks that matched their respective molecular formulas.

Antitubercular Activity

The synthesized compounds **3a–l and 4a-i** were evaluated for their in vitro antitubercular activity against the virulent *Mycobacterium tuberculosis* H37Rv strain using the broth microdilution method. [55–57]

The minimum inhibitory concentration (MIC) values were determined over a concentration range of 7.8–1000 µg/mL, using Rifampicin (1 µg/mL) as the reference drug and DMSO as the solvent control.[58–60] The obtained MIC values are summarized in Table 6. The screening results revealed that several compounds exhibited moderate inhibitory activity against the tested strain. Among the series, compounds 3k and 3l showed the most promising activity, with MIC values of 31.25

μg/mL, indicating superior inhibition compared with the other derivatives. Compounds 3f, 3i also demonstrated notable activity with MIC values of 62.5 μg/mL, whereas compounds 3b, 3c, 3h, 3j, 4b, 4d, 4e, 4f, 4g, 4i showed moderate inhibition (MIC = 125 μg/mL). In contrast, compounds 3a, 3d, and 3e exhibited weaker activity (MIC = 250 μg/mL), and 3g, 4c and 4h displayed very low activity with an MIC of 1000 μg/mL.

Overall, the results indicate that structural variations within the synthesized series significantly influence antitubercular potency, with compounds 3k and 3l emerging as the most active candidates of the present study. These findings suggest that the structural features present in these derivatives may contribute to improved interaction with the biological target of *M. tuberculosis*, highlighting them as promising scaffolds for further structural optimization and development of potential antitubercular agents.

On the other hand, the corresponding 9-Aryl-1,8-dioxo-octahydroxanthene derivatives were also synthesized from the dehydration and intramolecular cyclization of the tetraketone intermediates and subsequently evaluated for their *in vitro* antitubercular activity against *Mycobacterium tuberculosis* H37Rv. However, in contrast to the tetraketone series, the xanthene derivatives (4a-4i) exhibited only weak inhibitory activity, with MIC values of ≥125 μg/mL. We believe, this reduction in activity may be attributed to the rigid fused-ring xanthene framework, which likely decreases the availability of hydrogen-bonding functional groups and reduces conformational flexibility required for effective interaction with the biological target. These observations indicate that the tetraketone (diol) scaffold is more favorable for antitubercular activity than the corresponding cyclized xanthene derivatives.

A brief compound-based analysis suggests that variations in the aldehyde-derived aromatic moiety play a crucial role in modulating the antitubercular activity of the synthesized tetraketone derivatives against the H37Rv strain. Derivatives obtained from simple aromatic aldehydes (3a-3l) and (4a-4i) exhibited relatively weaker inhibitory activity, suggesting that mono-substituted phenyl frameworks provide only moderate interaction with the biological target. In contrast, derivatives derived from Terephthalaldehyde (3l and 3m) showed the most promising activity in the series. Notably, both the monomeric and dimeric tetraketone products exhibited significant inhibition with MIC values of 31.25 μg/mL, representing the highest

potency among the tested compounds. The improved activity of these derivatives may be attributed to the para-disubstituted aromatic framework, which provides greater molecular symmetry and an extended conjugated system. This structural arrangement may facilitate stronger π–π stacking and hydrophobic interactions with the biological target of *M. tuberculosis*. Additionally, the presence of multiple carbonyl and hydroxyl groups within the tetraketone scaffold may enhance hydrogen-bonding interactions with the active site residues, thereby stabilizing ligand–target binding.

Overall, these results suggest that terephthalaldehyde-derived architectures represent the most favorable structural motif within this series, highlighting them as promising lead structures for the further development of antitubercular agents.

Table 6: In vitro antitubercular activity of synthesized tetraketone **(3a–3l)** and xanthene **(4a–4i)** derivatives against M. tuberculosis H37Rv strain

Entry	Compound	MIC (µg/mL)
Tetraketone derivatives (Series 3)		
1	3a	250
2	3b	125
3	3c	125
4	3d	250
5	3e	250
6	3f	62.5
7	3g	1000
8	3h	125
9	3j	62.5
10	3k	31.25
11	3l	31.25
Xanthene derivatives (Series 4)		
12	4a	500

Entry	Compound	MIC (µg/mL)
13	4b	125
14	4c	1000
15	4d	125
16	4e	125
17	4f	125
18	4g	125
19	4h	1000
20	4i	125

[a] MIC = minimum inhibitory concentration; values reported in µg/mL.

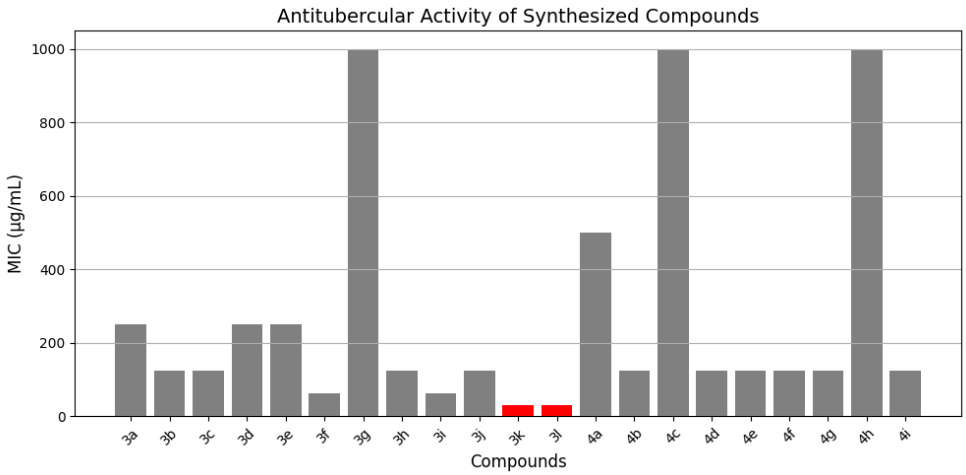


Fig 1: Graphical representation of antitubercular activity of compounds 3a–l and 4a–i against *Mycobacterium tuberculosis* H37Rv

Molecular docking

The present investigation primarily targets anti-tubercular activity, efforts were made to elucidate the interaction mechanisms of the most promising compounds through a combination of *in silico* computational approaches and experimental validation. Accordingly, molecular docking studies were incorporated to complement the biological evaluation of the observed activity. The synthesized compounds (3a–3l and 4a–4i) were subjected to molecular docking analysis against the *Mycobacterium tuberculosis* H37Rv strain, employing validated docking protocols to assess their binding interactions with the selected target protein.[61,62] The tetraketone and xanthene derived scaffolds were specifically analysed to rationalize

their biological potential at the molecular level. The reliability of the docking methodology was supported by consistency between computational predictions and experimental findings. Furthermore, the *in vitro* anti-tubercular screening revealed that compounds 3k and 3l exhibited superior activity against H37Rv. In agreement with these observations, docking results (Table 7) demonstrated significant binding affinities, with calculated binding energies ranging from –6.7 to –8.8 kcal/mol. The corresponding root-mean-square deviation (RMSD) values were found to lie within the range of 2.0 –3.6 Å, indicating acceptable conformational stability and reliable ligand–protein interactions.[63]

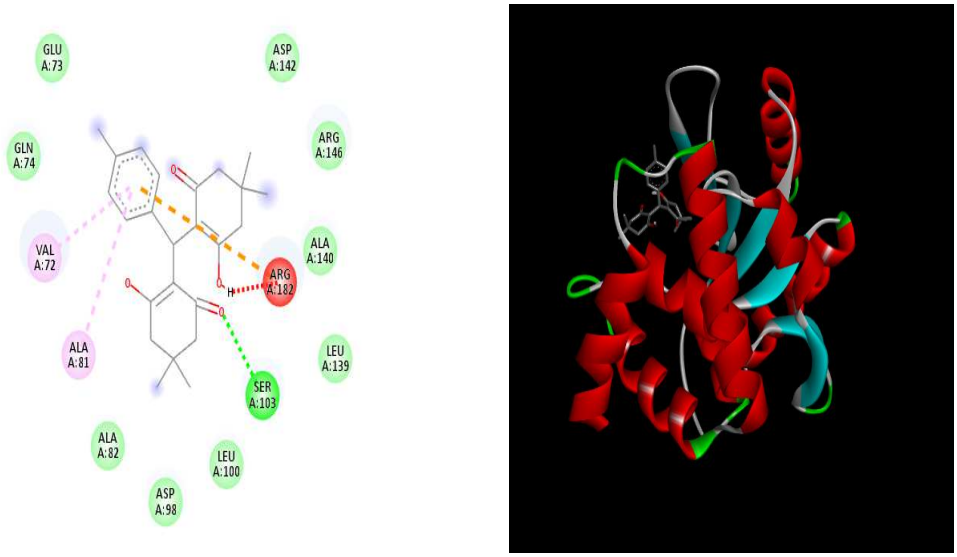


Fig 2: 2D and 3D binding interactions of compound **(3k)** with the targeted H37Rv. The figure illustrates key interactions between **(3k)** and specific amino acids in the binding site interactions.

Table 7: In silico docking results of synthesized compounds (3a–3l) and (4a-4i) against H37Rv

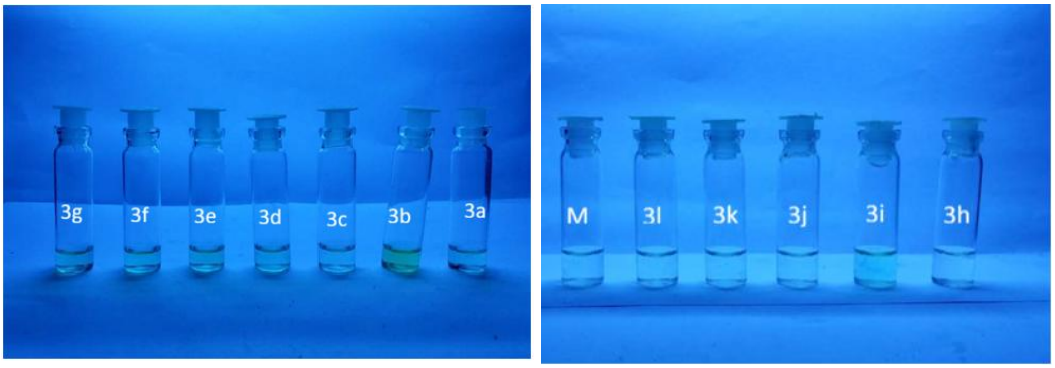
Ligand	Binding Affinity	rmsd/ub	rmsd/lb
PDB_8AN_**3a**_uff_E=296.85	-7.2	2.252	0.164
PDB_8AN_**3b**_uff_E=387.38	-6.9	12.64	8.618
PDB_8AN_**3c**_uff_E=285.09	-8.2	6.345	1.594
PDB_8AN_**3d**_uff_E=447.81	-6.7	36.4	32.64
PDB_8AN_**3e**_uff_E=367.96	-6.1	2.152	0.202
PDB_8AN_**3f**_uff_E=245.89	-7.9	27.45	24.28
PDB_8AN_**3g**_uff_E=247.73	-7.3	27.57	24.28
PDB_8AN_**3h**_uff_E=290.01	-7.7	27.45	24.45

PDB_8AN_**3i**_uff_E=528.72	-6.8	16.08	13.53
PDB_8AN_**3j**_uff_E=255.16	-7.9	6.519	1.953
PDB_8AN_**3k**_uff_E=254.58	-8.8	36.08	33.15
PDB_8AN_**3l**_uff_E=293.58	-8.8	5.183	1.604
8AN5_new_**4a**_uff_E=317.24	-7.4	15.713	12.408
8AN5_new_**4b**_uff_E=303.24	-7.6	21.51	18.329
8AN5_new_**4c**_uff_E=470.25	-7.1	17.321	14.618
8AN5_new_**4d**_uff_E=352.27	-7.2	22.867	20.379
8AN5_new_**4e**_uff_E=382.03	-7.3	5.494	1.588
8AN5_new_**4f**_uff_E=548.32	-7.4	2.316	0.06
8AN5_new_**4g**_uff_E=321.74	-7.4	16.128	13.074
8AN5_new_**4h**_uff_E=299.83	-7.6	6.127	2.437
8AN5_new_**4i**_uff_E=300.95	-7.3	6.266	2.446

Sensor studies

The sensing capability of the synthesized compounds (3a–3l) toward various inorganic cations was systematically evaluated using their corresponding nitrate salts, including K^{+}, Ca^{2+}, Mn^{2+}, Co^{2+}, Ni^{2+}, Cu^{2+}, Zn^{2+}, Fe^{3+}, Hg^{2+}, Sn^{2+}, Cd^{2+} and Al^{3+}. Initial screening was carried out through a visual fluorescence method under UV irradiation (λ = 350 nm). In this procedure, 10 μL of each analyte solution was introduced into 2 mL of the respective compound solution, and the resulting fluorescence response was monitored (Fig. 4). Among the tested metal ions, a distinct and selective response was observed exclusively in the presence of Fe^{3+} ions, demonstrating the high selectivity of the compounds toward this analyte. Notably, compound 3b exhibited a pronounced fluorescence quenching upon interaction with Fe^{3+} ions. Under UV illumination, the 3b–Fe^{3+} system displayed a significant "turn-off" response, manifested as a dark fluorescence signal, indicating efficient complex formation and strong quenching behaviour .[64,65]

a)



b)

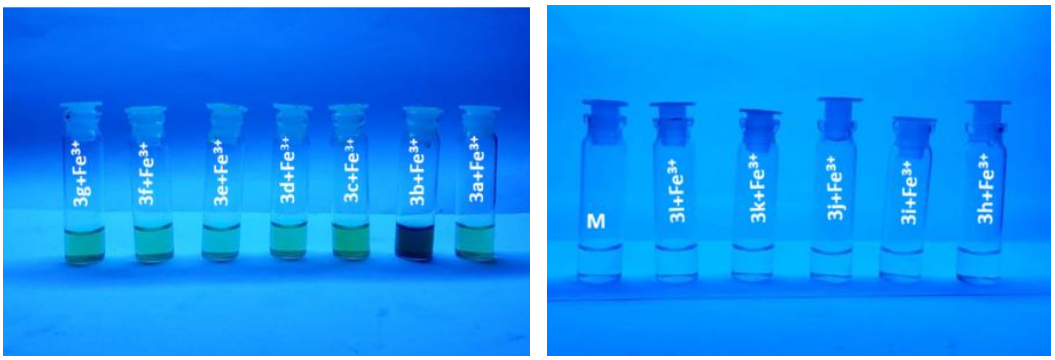


Fig 3: Visual responses of 3a-3l under UV light a) without addition of metal ions b) with addition of Fe^{3+} cations.

Fluorescence spectral studies

To gain comprehensive insight into the sensing behaviour of the synthesized compounds (3a–3l), detailed fluorescence spectroscopic investigations were carried out in the presence of various metal cations. The emission properties of all compounds were examined upon excitation at 350 nm, and the corresponding fluorescence spectra were recorded in the range of 400–550 nm. The addition of different metal ions revealed that most analytes produced negligible changes in fluorescence intensity. In contrast, upon addition of Fe^{3+} ions resulted in a marked quenching of emission, particularly at 414 nm. This pronounced decrease in fluorescence intensity is attributed to a chelation-enhanced quenching (CHEQ) mechanism arising from strong coordination interactions between Fe^{3+} ions and the ligand framework. Among the series, compound 3b exhibited the most significant response toward Fe^{3+} ions, displaying the highest degree of fluorescence quenching compared to the other derivatives. The remaining compounds showed minimal or no observable changes, highlighting the superior selectivity of 3b for Fe^{3+} detection. The selective "turn-off" fluorescence response of compound 3b can be ascribed to

effective coordination of Fe^{3+} ions with the available chelating sites, particularly involving the hydroxyl (–OH) functional groups. This interaction facilitates non-radiative decay pathways, leading to efficient quenching of fluorescence. These findings clearly establish 3b as a highly selective and sensitive probe for Fe^{3+} ions among the investigated compounds. [66]

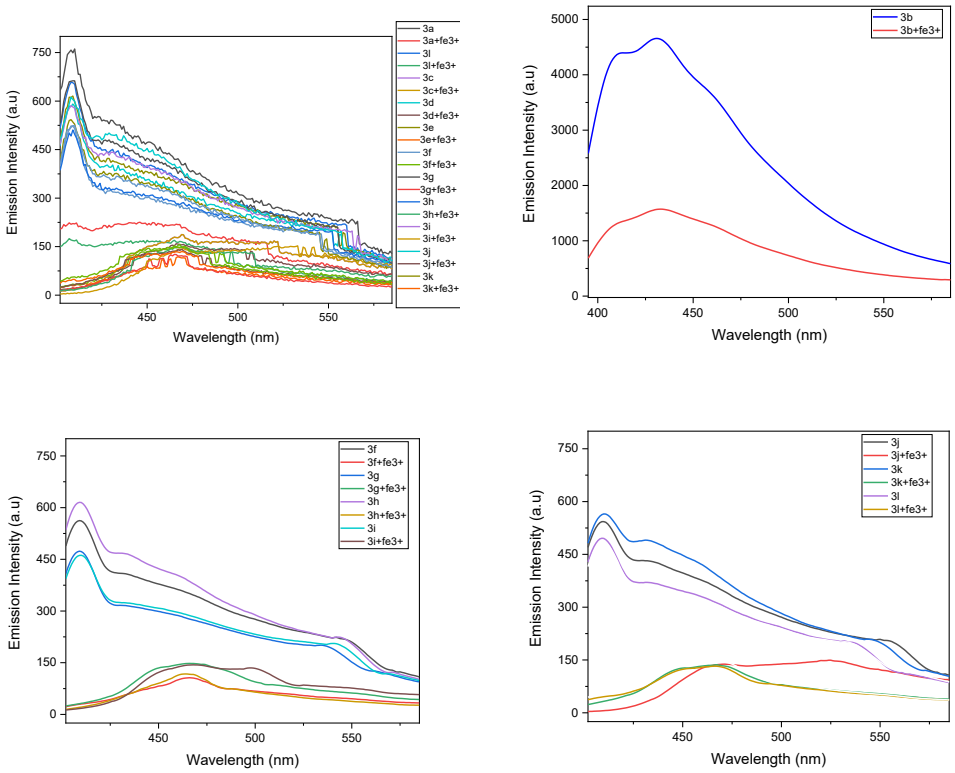


Fig 4: Fluorescence spectral changes of the chemosensors upon the addition of compounds and Fe^{3+} cations.

Conclusion

Overall, a sustainable and convenient protocol has been established for the preparation of tetraketone (3a-3l) and cyclised xanthene (4a-4i) derivatives by means of aspartic acid (30 mol%) as a renewable organocatalyst in water at ambient temperature. The dual Brønsted acidic and hydrogen-bonding functionalities of aspartic acid were essential for facilitating the efficient condensation under mild aqueous reaction conditions, avoiding the use of toxic chemicals and/or high temperatures. The reaction showed good tolerance towards both electron-rich and electron-deficient aromatic aldehyde substrates, providing the desired products in good to excellent yields.

Screening against M. tuberculosis H37Rv identified the tetraketone series as more active than the xanthene series in anti-tubercular activity. 3k and 3l were identified as the most potent with an MIC of 31.25 μg/mL, and a number of other tetraketones demonstrated moderate activity. The weaker activity of the xanthene series (MIC ≥ 125 μg/mL) suggests the importance of the open-chain tetraketone structure as the essential pharmacophore, which should be further explored in new anti-TB drug development. Apart from their pharmacological potential, compounds **3a-3l** were evaluated as fluorescent sensor probes for metal ions. Fluorescence titrations (λex = 350 nm) with twelve inorganic metal ions revealed that compound **3b** is a selective turn-off sensor for Fe^{3+}, displaying a marked decrease in emission intensity at 414 nm, free from interference by other cations. The selectivity is explained by the efficient coordination of Fe^{3+} at the chelating sites (containing multiple hydroxyl groups) of **3b**, which leads to non-radiative decay via a chelation-enhanced quenching (CHEQ) process. Selective Fe^{3+} sensing is important as iron metabolism is involved in many regulatory physiological and environmental processes.

On the whole, this study highlights the tetraketone scaffold as a structurally flexible and multifunctional scaffold, which holds promise in the development of both an anti-tubercular pharmacophore and a selective fluorescent probe for Fe^{3+} detection. The application of a naturally abundant amino acid catalyst in water also makes this process more environmentally sustainable, and an appealing strategy for future drug discovery and materials chemistry.

Materials and methods

Commercially available reagents and solvents were employed in this study after suitable purification to ensure the removal of possible contaminants prior to use. Structural characterization of the synthesized tetraketone and xanthene derivatives was accomplished through a combination of spectroscopic and analytical methods, namely Fourier transform infrared (FT-IR), nuclear magnetic resonance (NMR), high-resolution mass spectrometry (HRMS), and fluorescence spectroscopy. Infrared spectra were collected with a JASCO FT/IR-4100 spectrometer. Proton (^{1}H) NMR spectra were recorded on Bruker AVANCE instruments operating at 400 and 500 MHz, whereas carbon (^{13}C) NMR spectra were obtained on Bruker AVANCE spectrometers operating at 100 and 126 MHz under broadband proton-decoupled conditions. Chemical shift values (δ) are expressed in parts per million (ppm) using

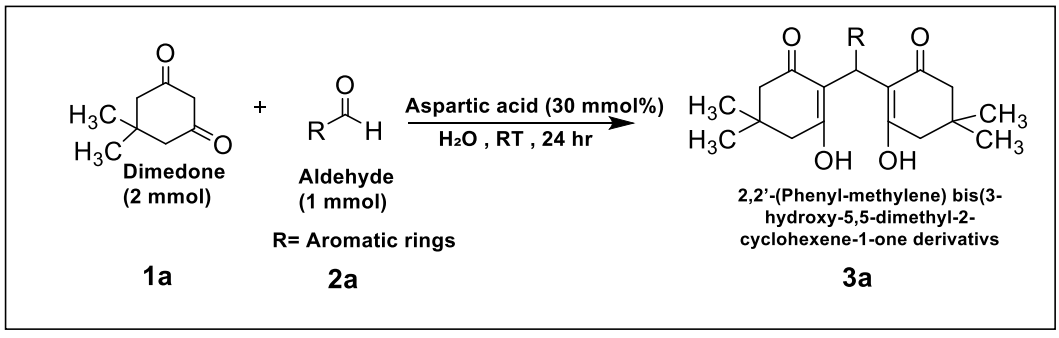
the residual $CDCl_3$ resonances (δ_H = 7.26 ppm and δ_C = 77.16 ppm) as internal references or tetramethylsilane (TMS, δ = 0.00 ppm) where applicable. High-resolution mass spectral analyses were carried out by electrospray ionization (ESI) using a Q-TOF Micro mass spectrometer fitted with a LockSpray ionization source. The progress of each reaction and the purity of the isolated compounds were routinely examined by thin-layer chromatography (TLC) on Merck silica gel 60 F_{254} aluminium-backed plates (0.25 mm thickness), with spot detection performed under ultraviolet illumination at wavelengths of 254 and 366 nm. Fluorescence emission measurements were performed using a SHIMADZU RF-6000 spectrofluorophotometer.

EXPERIMENTAL SECTION

GENERAL PROCEDURE AT ROOM TEMPERATURE

Synthesis of 2,2'-aryl-methylene bis(3-hydroxy-5,5-dimethyl-2-cyclohexene-1- one) derivatives

In a 15ml vial, a mixture of 0.5606g (4mmol) of dimedone, 10 ml of water and (30mol%) of aspartic acid was stirred at room temperature. 2mmol of aldehyde was then added and the reaction mixture was stirred for 24hr at same temperature. After completion of the reaction (monitored by TLC, (EA: Hexane-1:1)), water insoluble product was obtained and it was collected by filtration. Then the product was washed with water- ethanol mixture (80:20) to remove the unreacted starting materials and dried, gave the pure product in good yield. Appearance and melting point of the product was noted.



Synthesis of 2,2'-(Phenyl-methylene) bis(3-hydroxy-5,5-dimethyl-2- cyclohexene-1-one): 3a

Yellowish white solid, 85% (0.632g) ^{1}H NMR (500 MHz, $CDCl_3$) δ 11.90 (s, 1H, OH), 7.28-7.23 (d, 2H, ArH), 7.17 -7.14 (m, 1H, ArH), 7.10-7.08 (d ,2H, ArH), 5.54 (s, 1H, CH), 2.48-2.28 (m, 8H, CH_2), 1.23 (s, 6H, CH_3), 1.09 (s, 6H, CH_3) ppm. ^{13}C NMR (100 MHz, CDCl3) δ 190.48, 189.41, 138.09, 128.42, 128.23, 126.80, 125.85, 115.60, 77.41, 77.30, 77.09, 76.78, 47.08, 46.47, 32.77, 31.44, 29.66, 27.44 ppm. IR (neat): 2961, 1739, 1584, 1370, 1243, 1040, 844, 693, 576 cm^{-1}. HRMS (ESI) m/z: $[M+H]^+$ Calculated for $C_{23}H_{29}O_4^+$ 368.2060; found 368.2043. TLC: Rf =0.83 (EA: Hexane-1:1).

Synthesis of 9-(2-hydroxy-4,4-dimethyl-6-oxocyclohex-1-en-1-yl)-3,3-dimethyl-2,3,4,9-tetrahydro-1H-xanthen-1-one: 3b

Yellowish white solid, 79% (0.610g) ^{1}H NMR (500 MHz, $CDCl_3$): δ 10.58 (s, 1H, OH), 7.01-7.28 (m, 4H, ArH), 4.69 (s, 1H, CH), 2.63-2.46 (q, 2H, CH_2), 2.38-2.34 (m, 4H, CH_2), 1.98 (s, 2H, CH_2), 1.13 (s, 3H, CH_3), 1.03 (, 3H, CH_3),1.00 (s, 6H, CH_3) ppm. ^{13}C NMR (100 MHz, $CDCl_3$) δ 200.86, 196.76, 170.89, 169.12, 151.00, 128.03, 127.52, 124.59, 124.33, 118.32, 115.74 ,111.04, 77.52, 77.09, 76.67, 50.56, 49.94, 43.18, 41.54, 32.30, 30.99, 29.84, 29.19, 27.72, 27.19, 26.52 ppm. IR (neat): 3743, 2962, 1612, 1369, 1230, 1024, 752, 589 cm^{-1}. HRMS (ESI) m/z: $[M+H]^+$ Calculated for $C_{23}H_{27}O_4^+$ 367.1904; found 367.1892. TLC: Rf =0.80 (EA: Hexane-1:1).

Synthesis of 2,2'-((4-hydroxy-3,5-dimethoxyphenyl)methylene)bis(3-hydroxy- 5,5-dimethylcyclohex-2-en-1-one): 3c

Pure white solid **,** 80% (0.710g) ^{1}H NMR (500 MHz, $CDCl_3$): δ 12.01 (s, 1H, OH), 6.35 (s, 2H, ArH), 5.50(s, 1H, CH), 3.77 (s, 6H, OCH3), 2.43 – 2.35 (m, 8H, CH2),1.24 (s, 6H, CH_3), 1.12 (s, 6H, CH_3) ppm. ^{13}C NMR (100 MHz, $CDCl_3$): δ 190.33, 189.29, 146.80, 132.74, 129.08, 115.70, 103.96, 56.09,47.13 ,46.36, 32.55, 31.13, 29.99, 26.85 ppm. IR (neat): 2955, 1739, 1584, 1452, 1370, 1211, 1113, 1043, 829, 576 cm^{-1}. HRMS (ESI) m/z: $[M+H]^+$ Calculated for $C_{25}H_{32}O_7^+$ 445.2221; found 445.2217. TLC: Rf =0.81 (EA: Hexane-1:1).

Synthesis of 2,2'-((3,4-dimethoxyphenyl) methylene) bis(3-hydroxy-5,5-dimethylcyclohex-2-en-1-one): 3d

Pure white solid , 86% (0.710g) ^{1}H NMR (500 MHz, $CDCl_3$) δ 11.89 (s, 1H, OH), 6.70 (d,1H, ArH), 6.57 (d, 2H, ArH), 5.44(s, 1H, CH), 3.79 -3.78 (s, 6H, OCH_3), 2.36 – 2.23 (m, 8H, CH_2), 1.17 (s, 6H, CH_3), 1.04 (s, 6H, CH_3) ppm. ^{13}C NMR (100 MHz, $CDCl_3$): δ 210.67, 190.56, 189.86, 148.70, 147.10, 130.47, 118.90, 115.77, 110.97, 110.54, 55.86, 55.68, 47.11, 46.41, 32.31, 31.23, 29.86, 27.09 ppm. IR (neat): 2959, 1583, 1513, 1456, 1366, 1305, 1244, 1149, 1024, 879, 755, 662, 569cm^{-1}. HRMS (ESI) m/z:

$[M+H]^+$ Calculated for $C_{25}H_{33}O_6^+$ 429.2272; found 429.2269. TLC: Rf =0.83 (EA: Hexane-1:1).

Synthesis of 2,2'-((4-(dimethylamino)phenyl)methylene)bis(3-hydroxy-5,5-dimethylcyclohex-2-en-1-one): 3e

Pure yellow solid, 81% (0.665g) ^{1}H NMR (500 MHz, $CDCl_3$) δ 11.92 (s, 1H, OH), 6.95 -6.93 (d, 2H, ArH), 6.67 -6.65 (d, 2H, ArH), 5.47 (s, 1H, CH), 2.90 (s, 6H, CH_3), 2.45 – 2.29 (m, 8H, CH_2), 1.22 (s, 6H, CH_3), 1.09 (s, 6H, CH_3) ppm. ^{13}C NMR (100 MHz, $CDCl_3$): δ 190.21, 189.26, 148.79, 127.49, 125.64, 115.97, 112.70, 47.11, 46.48, 40.71, 31.86, 31.38, 29.69, 27.36 ppm. IR (neat): 2959, 1583, 1513, 1456, 1366, 1305, 1244, 1149, 1024, 913, 808, 662, 569cm^{-1}. HRMS (ESI) m/z: $[M+H]^+$ Calculated for $C_{25}H_{34}NO_4^+$ 412.2482; found 412.2464. TLC: Rf =0.85 (EA: Hexane-1:1).

Synthesis of 2,2'-((3,4-dihydroxyphenyl)methylene)bis(3-hydroxy-5,5-dimethylcyclohex-2-en-1-one): 3f

Half grey solid, 87% (0.670g) ^{1}H NMR (500 MHz, $CDCl_3$) δ 11.92 (s, 1H, OH), 6.76 -6.74 (d, 1H, ArH), 6.62 (s, 1H, ArH) 6.54 -6.52 (d, 1H, ArH), 5.47 (s, 1H, CH), 2.48 – 2.30 (m, 8H, CH_2), 1.24 (s, 6H, CH_3), 1.11 (s, 6H, CH3) ppm. ^{13}C NMR (100 MHz, $CDCl_3$): δ 194.71, 179.75, 151.16, 134.34, 130.03, 129.03, 119.25, 115.73, 115.17, 114.45, 111.43 , 53.02, 47.13, 32.11, 31.46, 29.53, 27.53 ppm. IR (neat): 3471, 2965, 1583, 1371, 1262, 1157, 1059, 952, 868, 775, 662, 599cm^{-1}. HRMS (ESI) m/z: $[M+H]^+$ Calculated for $C_{23}H_{29}O_6^+$ 401.1959; found 401.1947. TLC: Rf =0.80 (EA: Hexane-1:1).

Synthesis of 2,2'-((4-hydroxy-3-methoxyphenyl)methylene)bis(3-hydroxy-5,5-dimethylcyclohex-2-en-1-one): 3g

Half white solid, 77% (0.640g) ^{1}H NMR (500 MHz, $CDCl_3$) δ 11.95 (s, 1H, OH), 6.81 -6.61 (d, 1H, ArH), 6.59 -6.56 (d, 2H, ArH), 5.49 (s, 1H, CH), 3.76 (s, 3H, OCH_3), 2.47 – 2.29 (m, 8H, CH2), 1.23 (s, 6H, CH_3), 1.11 (s, 6H, CH_3) ppm ^{13}C NMR (100 MHz, $CDCl_3$) δ 190.39, 189.36, 146.34, 143.61, 129.75, 119.53, 115.80, 114.11 , 109.87, 55.68, 47.10, 46.41, 32.33, 31.26, 29.82, 27.11 ppm. IR (neat): 3514, 2955, 1590, 1510, 1369, 1243, 1155, 1032, 861 cm^{-1}. HRMS (ESI) m/z: $[M+H]^+$ Calculated for $C_{24}H_{31}O_6^+$ 415.2115; found 415.2079. TLC: Rf =0.82 (EA: Hexane-1:1).

Synthesis of 2,2'-((3,4,5-trimethoxyphenyl)methylene)bis(3-hydroxy-5,5-dimethylcyclohex-2-en-1-one): 3h

Pure white solid ,74% (0.680g) ^{1}H NMR (500 MHz, $CDCl_3$) δ 12.02 (s, 1H, OH), 6.36 (s, 2H, ArH), 5.50 (s, 1H, CH), 3.81 (s, 3H, OCH_3) , 3.76 (s, 6H ,OCH_3) , 2.36-2.41 (m, 8H, CH_2), 1.25 (s, 6H, CH_3), 1.12 (s, 6H, CH_3) ppm. ^{13}C NMR (100 MHz, $CDCl_3$) δ 190.40 , 189.31, 152.84, 135.94, 133.76, 115.52 ,104.21, 77.43, 77.11, 76.79, 60.84, 55.92, 47.09, 46.32, 32.77, 31.10, 29.99, 26.81 ppm. IR (neat): 2947, 1580, 1508, 1369, 1238, 1126, 1010, 885, 827 cm^{-1}.HRMS (ESI) m/z: $[M+H]^+$ Calculated for $C_{26}H_{35}O_7^+$ 459.2377; found 459.2374. TLC: Rf =0.85 (EA: Hexane-1:1).

Synthesis of 2,2'-((4-chlorophenyl)methylene)bis(3-hydroxy-5,5-dimethylcyclohex-2-en-1-one) : 3i

Pure white solid ,82% (0.660g) ^{1}H NMR (500 MHz, $CDCl_3$) δ 11.86 (s, 1H, OH), 7.23-7.21 (d , 2H, ArH), 7.02-7.00 (d ,2H, ArH) 5.47 (s, 1H, CH), 2.48-2.29 (m, 8H, CH_2), 1.22 (s, 6H, CH_3), 1.10 (s, 6H, CH_3) ppm. ^{13}C NMR (100 MHz, $CDCl_3$): δ 190.63, 189.43, 136.71, 131.60, 128.35, 128.20, 115.34, 47.06, 46.44, 32.41, 31.43, 29.58, 27.42 ppm. IR (neat): 2962, 1580, 1366, 1253, 1157, 874, 587 cm^{-1}. HRMS (ESI) m/z: $[M+H]^+$ Calculated for $C_{23}H_{28}CLO_4^+$ 403.1671; found 403.1650. TLC: Rf =0.79 (EA: Hexane-1:1).

Synthesis of 2,2'-(p-tolylmethylene)bis(3-hydroxy-5,5-dimethylcyclohex-2-en-1-one): 3j

Pure white solid, 83% (0.690g) ^{1}H NMR (500 MHz, $CDCl_3$) δ 11.90 (s, 1H, OH), 7.08 -7.06 (d, 2H, ArH), 6.96 (d, 2H, ArH), 5.50 (s, 1H, CH), 2.47-2.32 (m, 8H, CH2) 1.22 (s, 6H, CH3), 1.09 (s, 6H, CH_3),1.03 (s, 3H, CH_3) ppm. ^{13}C NMR (100 MHz, $CDCl_3$) δ 203.68, 190.43, 189.43, 134.92, 130.15, 128.96, 126.68, 115.73, 103.63, 57.33, 54.12, 47.08, 46.32, 32.45, 31.47, 30.93, 29.64, 28.38, 28.35, 27.41, 20.90 ppm. IR (neat): 2953, 1592, 1458, 1369, 1241, 1157, 1030, 879, 810, 653 cm^{-1}. HRMS (ESI) m/z: $[M+H]^+$ Calculated for $C_{24}H_{31}O_4^+$ 383.2217; found 383.2204. TLC: Rf =0.84 EA: Hexane-1:1).

Synthesis of 2,2',2'',2'''-(1,4-phenylenebis(methanetriyl))tetrakis(3-hydroxy- 5,5-dimethylcyclohex-2-en-1-one): 3k

Pure white solid, 82% (0.650g) ^{1}H NMR (500 MHz, $CDCl_3$) δ 11.82 (s, 2H, OH), 9.96 (s, 1H, OH), 7.26-7.80 (s, 4H, ArH), 5.56 (s, 2H, CH), 2.47-2.35 (m, 16H, CH_2), 1.24 (s, 12H, CH_3), 1.11 (s, 12H, CH_3) ppm. ^{13}C NMR (100 MHz, $CDCl_3$) δ 191.68, 190.75, 189.52, 145.94, 134.39, 129.75, 127.45, 126.74, 115.16 ,77.24, 47.04, 46.44, 33.36, 31.49, 31.46, 29.53, 27.48 ppm. IR (neat): 2959, 1685, 1589, 1377, 1247, 1160, 1050, 877, 668 cm^{-1}. HRMS (ESI) m/z: $[M+H]^+$ Calculated for $C_{40}H_{51}O_8^+$ 659.3578; found 659.3578. TLC: Rf =0.86 EA: Hexane-1:1).

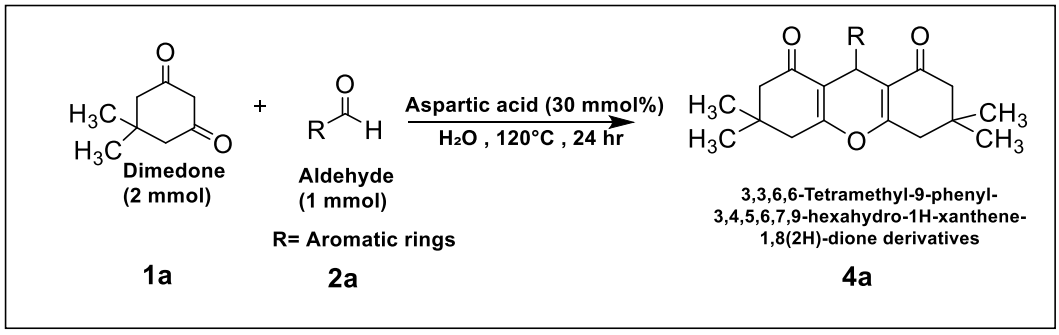
Synthesis of 4-(bis(2-hydroxy-4,4-dimethyl-6-oxocyclohex-1-en-1-yl)methyl)benzaldehyde: 3l

Pure white solid, 84% (0.670g) ^{1}H NMR (500 MHz, $CDCl_3$) δ 11.83 (s, 1H, OH), 9.96 (s, 1H, CHO), 7.25-7.80 (s, 4H, ArH), 5.56 (s, 1H, CH), 2.31-2.53 (m, 8H, CH_2), 1.24 (s, 6H, CH_3), 1.11 (s, 6H, CH_3) ppm. ^{13}C NMR (100 MHz, $CDCl_3$) δ 191.72, 190.78, 189.55, 145.95, 134.38, 129.77, 127.45, 115.16, 77.24, 47.03, 46.44, 33.36, 31.49, 29.56, 27.47 IR (neat): 2962, 1693, 1583, 1369, 1299, 1163, 1050, 871, 668 cm^{-1}.HRMS (ESI) m/z: $[M+H]^+$ Calculated for $C_{24}H_{29}O_5^+$ 397.2010; found 397.2005. TLC: Rf =0.82(EA: Hexane-1:1).

GENERAL PROCEDURE OF B AT HOT TEMPERATURE

Synthesis of 3,3,6,6-Tetramethyl-9-phenyl-3,4,5,6,7,9-hexahydro-1H-xanthene-1,8(2H)-dione derivatives

In a 50 ml Rb flask, a mixture of 0.5606g (4 mmol) of dimedone, 10 ml of ethanol and (30 mol%) of aspartic acid was stirred at 120°C temperature. 204.06 µl (2 mmol) of aldehyde was added then the reaction mixture was stirred for 24hr at same temperature. After completion of the reaction (monitored by TLC, EA: Hexane-1:1), water insoluble product was obtained and it was collected by filtration. Then the product was washed with water- ethanol mixture (80:20) to remove the unreacted starting materials and dried, gave the pure product in good yield. Appearance and melting point of the product was noted.



Synthesis of 3,3,6,6-Tetramethyl-9-phenyl-3,4,5,6,7,9-hexahydro-1H-xanthene-1,8(2H)-dione: 4a

White solid ,85% (0.632g) ^{1}H NMR (500 MHz, $CDCl_3$) δ 7.32- 7.29 (d, 2H,ArH), 7.25 -7.20 (t, 2H,ArH), 7.14-7.11 (d ,1H,ArH) 4.76 (s, 1H, CH), 2.48-2.15 (m, 8H, CH_2), 1.12 (s, 6H, CH_3), 1.01 (s, 6H, CH_3) ppm.^{13}C NMR (100 MHz, $CDCl_3$) δ 196.32, 162.22, 144.09,128.52, 128.39, 128.04, 126.37, 115.71, 77.33,77.02, 76.70, 50.77, 40.91, 32.19, 31.84, 29.26, 27.35 ppm. IR (neat): 2959, 1658, 1595, 1360, 1195, 1140, 1001, 697 cm^{-1}.HRMS (ESI) m/z: $[M+H]^+$ Calculated for $C_{23}H_{27}O_3^+$ 351.1955; found 351.1967. TLC : Rf =0.84(EA: Hexane-1:1).

Synthesis of 9-(2-hydroxy-4,4-dimethyl-6-oxocyclohex-1-en-1-yl)-3,3-dimethyl-2,3,4,9-tetrahydro-1H-xanthen-1-one: 4b

Yellowish white solid, 82% (0.630g) ^{1}H NMR (500 MHz, $CDCl_3$) δ 10.58 (s, 1H, OH), 7.01-7.28 (m, 4H, ArH), 4.69 (s, 1H, CH), 2.63-2.46 (q, 2H, CH_2), 2.38-2.34 (m, 4H, CH_2), 1.98 (s, 2H, CH_2), 1.13 (s, 3H, CH_3), 1.03 (, 3H, CH_3),1.00 (s, 6H, CH_3), ppm. ^{13}C NMR (100 MHz, $CDCl_3$) δ 200.86, 196.76, 170.89, 169.12, 151.00, 128.03, 127.52, 124.59, 124.33, 118.32, 115.74 ,111.04, 77.52, 77.09, 76.67, 50.56, 49.94, 43.18, 41.54, 32.30, 30.99, 29.84, 29.19, 27.72, 27.19, 26.52 ppm. IR (neat): 3743, 2962, 1612, 1369, 1230, 1024, 752, 589 cm^{-1}. HRMS (ESI) m/z: $[M+H]^+$ Calculated for $C_{23}H_{27}O_4^+$ 367.1904; found 367.1892. TLC: Rf =0.85 (EA: Hexane-1:1).

Synthesis of 9-(4-Hydroxy-3-methoxyphenyl)-3,3,6,6-tetramethyl-3,4,5,6,7,9-hexahydro-2H-xanthene-1,8-dione : 4g

Pure white solid, 71% (0.610g) ^{1}H NMR (500 MHz, $CDCl_3$) δ 6.92 (s, 1H, OH), 6.66-6.64 (s, 1H, ArH), 6.52-6.50 (d, 1H, ArH), 5.59 (s, 1H, ArH), 4.59 (s, 1H, CH), 3.80 (s, 3H, OCH_3), 2.38 (s, 4H, CH_2), 2.18 -2.04 (m, 4H, CH_2), 1.02 (s, 6H, CH_3), 0.93 (s, 6H, CH_3) ppm. ^{13}C NMR (100 MHz, $CDCl_3$) δ 196.71, 162.63, 162.18, 145.96, 144.06, 136.42, 120.08, 115.81, 114.00, 112.29, 77.28, 55.92, 55.89, 50.76, 45.97, 40.86, 36.51, 32.19, 32.04, 31.46, 31.30, 29.29, 27.27 ppm. IR (neat): 3405, 2959, 1661, 1510, 1354, 1201, 1027, 813 cm^{-1}. HRMS (ESI) m/z: $[M+H]^+$ Calculated for $C_{24}H_{29}O_5^+$ 397.2010; found 397.2009. TLC: Rf =0.81 (EA: Hexane-1:1).

Synthesis of 3,3,6,6-Tetramethyl-9-(3,4,5-trimethoxyphenyl)-3,4,5,6,7,9-hexahydro-1H-xanthene-1,8(2H)-dione: 4h

Pure white solid, 79% (0.670g) ^{1}H NMR (500 MHz, $CDCl_3$) δ 6.44 (s, 2H, ArH), 4.64 (s, 1H, CH), 3.73(s, 6H, OCH_3), 3.70 (s, 3H, OCH_3), 2.36 - 2.29 (m, 2H, CH_2), 2.22 -2.12 (dd, 6H, CH_2), 1.04 (s, 6H, CH_3), 0.96 (s, 6H, CH_3) ppm.^{13}C NMR (100 MHz, $CDCl_3$) δ 196.50, 190.38, 189.52, 189.30, 162.38, 152.83, 152.78, 139.74,136.57, 133.76, 115.55, 113.45, 105.73, 104.17, 77.30, 60.84, 60.68, 56.09, 55.89, 50.75, 47.10, 46.32, 45.98, 40.90, 32.27, 32.17, 32.03, 31.81, 31.10, 30.01, 29.36, 27.18 ppm.IR (neat): 2953, 1664, 1589, 1458, 1351, 1126, 1007, 833 cm^{-1}. HRMS (ESI) m/z: $[M+H]^+$ Calculated for $C_{26}H_{33}O_6^+$ 441.2272; found 441.2269. TLC : Rf =0.84 (EA: Hexane-1:1).

Synthesis of 9-(4-chlorophenyl)-3,3,6,6-tetramethyl-3,4,5,6,7,9-hexahydro-1H-xanthene-1,8(2H)-dione : 4i

Pure white solid, 79% (0.640g) ^{1}H NMR (500 MHz, $CDCl_3$) δ 7.10-7.09 (d, 2H, ArH), 6.95-6.89 (dt ,2H, ArH), 4.63 (s, 1H, CH), 2.38 (s, 4H, CH_2), 2.16 -2.07 (m, 4H, CH_2), 1.02 (s, 6H, CH_3), 0.92 (s, 6H, CH_3) ppm. ^{13}C NMR (100 MHz, $CDCl_3$) δ 196.45, 162.13, 141.20, 135.77, 135.26, 134.93, 128.95, 128.79, 128.25, 126.67, 115.78, 115.74, 77.26, 50.79, 47.09, 46.46,

40.89, 32.42, 32.21, 31.45, 31.42, 29.27, 27.39, 21.06, 20.89 ppm. IR (neat): 2884, 1461, 1343, 1279, 1027, 952, 841 cm^{-1}.HRMS (ESI) m/z: $[M+H]^+$ Calculated for $C_{23}H_{26}CLO_3{}^+$ 385.1565; found 385.2281. TLC : Rf =0.81 (EA: Hexane-1:1).

Synthesis of 3,3,6,6-Tetramethyl-9-(p-tolyl)-3,4,5,6,7,9-hexahydro-1H-xanthene-1,8(2H)-dione: 4j

Pure white solid, 75% (0.640g) ^1H NMR (500 MHz, $CDCl_3$) δ 7.17-7.15 (d, 2H, ArH), 7.11-7.09 (d ,2H, ArH), 4.64 (s, 1H, CH), 2.36 - 2.22 (s, 4H, CH_2), 2.18 -2.07 (m, 4H, CH_2), 1.03 (s, 9H, CH_3), 0.91 (s, 6H, CH_3) ppm.^{13}C NMR (100 MHz, $CDCl_3$) δ 196.39, 190.64, 189.44, 162.48, 142.73, 136.75, 132.02, 131.56,129.79, 128.34, 128.21, 115.33, 77.28, 50.70, 47.05, 46.43, 40.85, 32.41, 32.21, 31.48, 31.43,29.58, 29.28, 27.43, 27.29 ppm. IR (neat): 2956, 1658, 1586, 1363, 1192, 1004, 841 cm^{-1}. HRMS (ESI) m/z: $[M+H]^+$ Calculated for $C_{24}H_{29}O_3{}^+$ 365.2111; found 365.2126. TLC : Rf =0.85 (EA: Hexane-1:1).

Synthesis of 4-(3,3,6,6-Tetramethyl-1,8-dioxo-2,3,4,5,6,7,8,9-octahydro- 1H-xanthene-9-yl) benzaldehyde : 4i

Pure white solid, 80% (0.635g) ^1H NMR (500 MHz, $CDCl_3$) δ 9.92 (s, 1H, CHO), 7.76- 7.74 (d, 2H, ArH), 7.49- 7.47 (d, 2H, ArH), 4.81 (s, 1H, CH), 2.49 (s, 4H, CH_2), 2.27-2.14 (m, 4H, CH_2), 1.11 (s, 6H, CH_3), 0.98 (s, 6H, CH_3) ppm. ^{13}C NMR (100 MHz, $CDCl_3$) δ 196.33, 192.06, 162.79, 151.06, 134.78, 129.73, 129.18, 114.84 ,77.26, 50.80, 50.68, 40.86, 32.47, 32.22, 29.27, 28.99, 27.24 ppm. IR (neat): 2962, 1661, 1497, 1353, 1275, 1133, 1040, 714, 697 cm^{-1}. HRMS (ESI) m/z: $[M+H]^+$ Calculated for $C_{24}H_{27}O_4{}^+$ 379.1904; found 379.1914. TLC : Rf =0.85 (EA: Hexane-1:1).

Antitubercular activity

Drugs and Chemical

Rifampicin (RMP) (Cat 557303), The dimethyl sulfamide (DMSO), Middle brook 7H9, OADC, were obtained from Himedia. The clear flat bottom microtiter 96 well plates (cat 980040) were obtained from Tarsons .

Maintenance of Mycobacterium tuberculosis strain and bacterial inoculum preparation

The laboratory strain Mycobacterium tuberculosis H37Rv (Mtb H37Rv) and clinical isolates were obtained from the ICMR–National Institute for Research in Tuberculosis (ICMR-NIRT), Chennai, India, and subcultured on Lowenstein–Jensen (LJ) medium. All in vitro experiments were carried out in the Biosafety Level 3 (BSL-3) laboratory of the Department of Bacteriology, ICMR-NIRT, Chennai, following the institute's standard operating procedures (SOPs).

The clinical isolates used in this study were obtained from the ICMR-NIRT culture repository. No human participants were recruited, and no patient interaction or collection of identifiable patient information was involved in this study. The study was conducted with the approval of the Institutional Ethics Committee of the National Institute for Research in Tuberculosis (Approval No. 031/NIRT-IEC/2019; NIRT-IEC ID: 2020 001) under the project entitled "Lead Generation for Drug-Resistant Tuberculosis."

The bacterial inoculum was prepared according to the standard protocol. Briefly, fresh three-week-old colonies of Mtb H37Rv and the clinical isolates were suspended in a Bijou bottle containing sterile glass beads and Middlebrook 7H9 broth (Difco, Detroit, MI, USA) supplemented with 10% (v/v) OADC (oleic acid, albumin, dextrose, and catalase; BD) and 0.2% glycerol. To disperse bacterial clumps, the suspension was vortexed and allowed to stand for 30 s to permit aerosol settlement. The supernatant was then carefully aspirated and adjusted to McFarland standard No. 1 (approximately 3×10^6 CFU/mL). The standardized inoculum was further diluted 1:20 in Middlebrook 7H9 medium supplemented with OADC by adding 0.5 mL of the bacterial suspension to 9.5 mL of the medium before use in the susceptibility assays. [67]

Anti-Mycobacterial Activity Test and Minimum Inhibitory Concentration Determination

The minimum inhibitory concentration (MIC) of 3a-3l against H37Rv was determined at concentrations ranging from 0.48 µg/ml to 1000 µg/ml. 100µl of 7H9 with 10% OADC and 0.2% of glycerol was dispensed in flat bottom 96 well plate, and the crude and fractions (100µl) were serially diluted (2-fold dilution) to obtain different concentrations.[67] Finally, 100µl of bacterial inoculum (1:20) was added to each well and incubated for 7 to 14 days, at 37 °C with 5% CO_2. The Mtb growth was evaluated by the direct microscopy method under the inverted microscope by observing the cord formation. All tests were performed in duplicate well and the assay was repeated twice the time. The MIC was defined as the lowest

concentration of plant extract that completely inhibited bacterial growth.[68] DMSO (0.2%) was used as a solvent control. Rifampicin (RMP) was used as a drug control (0.25µg/ml). The untreated culture was used as the growth control.

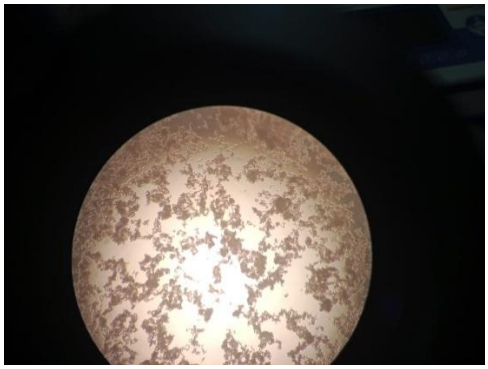


Fig 5: Chord formation by Mtb indicates that the compound lacks inhibitory activity

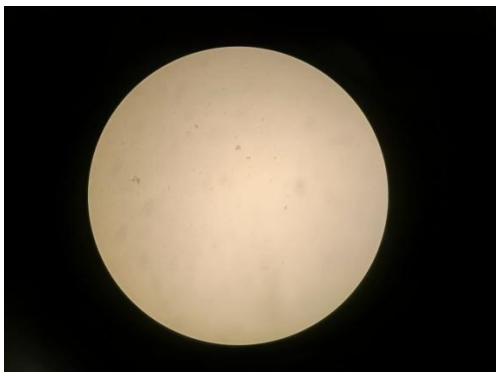


Fig 6: No Mtb growth indicates that the compound exhibits antimycobacterial activity.

Sensor studies

The preliminary detection of cations was carried out under UV light at 350 nm by naked eye colorimetric observation. Compounds with a concentration of 2.5 µM were prepared in Methanol. The cations with a concentration of 2.5 mM were prepared in deionized water, respectively. In order to check the noticeable colour changes of the compounds, 10 µL of cationic solution was added to the compounds.

General procedure for emission measurements

The compounds **(3a-3l)** were dissolved in Methanol to prepare the stock solution at a concentration of 2.5 mM, and further diluted with acetonitrile to a final concentration of 25 µM. To evaluate the selectivity of the compounds towards different ions, separate solutions

(2.5 mM) of cations were prepared in de-ionized water, respectively. The compounds (2 mL) were filled in a quartz cell with a 1-cm optical path length, and 5 μL of cations were added using a micropipette, after which UV-Vis and fluorescence spectra were recorded. For fluorescence titrations, the excitation wavelength was set at 350 nm. All titrations were carried out at room temperature.

Author contributions

A. Asif Shariff, E. Mohan Ram, and M. I. Abdul Bazith designed and performed the experimental work, including the synthesis and characterization of the compounds. A. K. Raees Ahmed carried out the fluorescence studies and contributed to the interpretation of the corresponding results. V. N. Azger Dusthackeer performed the anti-tuberculosis activity studies, interpreted the biological results, and contributed to writing the section describing the anti-tuberculosis activity. M. Ambrose Rajkumar and Sivakumar Sivalingam critically reviewed the manuscript and provided valuable scientific input. Habeebullah Thajudeen and V. S. Jamal Ahamed supervised the research, contributed to the interpretation of the results, and wrote and revised the manuscript. All authors reviewed the manuscript, approved the final version, and agree to be accountable for all aspects of the work.

Conflicts of interest

The authors declare that they have no known competing financial interests or personal relationships that could have appeared to influence the work reported in this paper.

Competing Interests

The authors declare that they have no competing interests.

Ethics Approval, Consent to Participate, and Consent for Publication

Ethics approval: Not applicable.

Consent to participate: Not applicable.

Consent for publication: Not applicable.

Funding

This research received no external funding.

Data availability

The data supporting this article have been included as part of the supplementary information (SI).

Acknowledgements

The authors acknowledge financial support from the Tamil Nadu State Government through a research scholar stipend (Rc. No. 00160/L/2022 dated 14.11.2023, Directorate of Collegiate Education, Chennai). The authors also thank the Management of The New College for providing SEED grant support and necessary research facilities.

References

1 K. Chibale, M. Visser, D. van Schalkwyk, P. J. Smith, A. Saravanamuthu and A. H. Fairlamb, *Tetrahedron*, 2003, **59**, 2289–2296.

2 G. M. Maharvi, S. Ali, N. Riaz, N. Afza, A. Malik, M. Ashraf, L. Iqbal and M. Lateef, *J. Enzyme Inhib. Med. Chem.*, 2008, **23**, 62–69.

3 K. M. Khan, G. M. Maharvi, M. T. H. Khan, A. Jabbar Shaikh, S. Perveen, S. Begum and M. I. Choudhary, *Bioorg. Med. Chem.*, 2006, **14**, 344–351.

4 M. Ahmad, T. A. King, D.-K. Ko, B. H. Cha and J. Lee, *J. Phys. D Appl. Phys.*, 2002, **35**, 303.

5 B. Das, M. Krishnaiah, K. Laxminarayana, K. Damodar and D. N. Kumar, *Chem. Lett.*, 2008, **37**, 1000–1001.

6 M. Saha, J. Dey, K. Ismail and A. K. Pal, *Lett. Org. Chem.*, 2011, **8**, 554–558.

7 H. Hagiwara, A. Numamae, K. Isobe, T. Hoshi and T. Suzuki, *MICROWAVE-PROMOTED SEQUENTIAL THREE-COMPONENT SYNTHESIS OF TETRAHYDROBENZO[b]PYRAN IN WATER CATLYZED BY HETEROGENEOUS AMINE GRAFTED ON SILICA*, 2006, vol. 68.

8 T.-S. Jin, J.-S. Zhang, J.-C. Xiao, A.-Q. Wang and T.-S. Li, *Synlett*, 2004, 0866–0870.

9 X. Fan, X. Hu, X. Zhang and J. Wang, *Can. J. Chem.*, 2005, **83**, 16–20.

10 S. Sudha and M. A. Pasha, *Ultrason. Sonochem.*, 2012, **19**, 994–998.

11 B. Das, J. Kashanna, R. A. Kumar and P. Jangili, *Synth. Commun.*, 2012, **42**, 2876–2884.

12 N. Azizi, E. Batebi, S. Bagherpour and H. Ghafuri, *RSC Adv.*, 2012, **2**, 2289.

13 J. M. KHURANA and K. VIJ, *Journal of Chemical Sciences*, 2012, **124**, 907–912.

14 J.-J. Yu, L.-M. Wang, J.-Q. Liu, F.-L. Guo, Y. Liu and N. Jiao, *Green Chem.*, 2010, **12**, 216–219.

15 E. Llama, *Eur. J. Med. Chem.*, 1989, **24**, 391–396.

16 K. Taheri, D. Elhamifar, S. Kargar and A. Zarnegaryan, *RSC Adv.*, 2023, **13**, 16067–16077.

17 *Biointerface Res. Appl. Chem.*, 2020, **10**, 6706–6717.

18 Z. Akhlaghi, M. R. Naimi-Jamal, L. Panahi, M. G. Dekamin and B. Farasati Far, *Heliyon*, 2023, **9**, e13522.

19 M. A. Zolfigol, A. Khazaei, A. R. Moosavi-Zare, J. Afsar, V. Khakyzadeh and O. Khaledian, *Journal of the Chinese Chemical Society*, 2015, **62**, 398–403.

20 K. K. Gangu, S. Maddila, S. B. Mukkamala and S. B. Jonnalagadda, *Ind. Eng. Chem. Res.*, 2017, **56**, 2917–2924.

21 P. G. Abrantes, P. G. Abrantes, R. R. Magalhães, F. S. C. Colaço, Y. V. Santos, G. C. G. Militão, E. E. S. Teotônio and J. A. Vale, *Research on Chemical Intermediates*, 2026, **52**, 461–480.

22 V. Galstyan, E. Comini, I. Kholmanov, G. Faglia and G. Sberveglieri, *RSC Adv.*, 2016, **6**, 34225–34232.

23 B. Li, T. Liu, Y. Wang and Z. Wang, *J. Colloid Interface Sci.*, 2012, **377**, 114–121.

24 F. S. Ghoreishi, V. Ahmadi and M. Samadpour, *Synthesis and Characterization of Graphene-ZnO Nanocomposite and its Application in Photovoltaic Cells*, 2013, vol. 3.

25 L. Huang, Y. Zhang, H. Liu, B. Liu and M. Tu, *New J. Chem.*, 2014, **38**, 5817–5824.

26 J. Griffiths and W. J. Lee, *Dyes and Pigments*, 2003, **57**, 107–114.

27 S. Ponnampalli and N. V. S. Birudukota, *Health Sciences Review*, 2023, **9**, 100128.

28 V. Singh, *Drug Discov. Today*, 2024, **29**, 103955.

29 A. A. Velayati, P. Farnia and A. M. Farahbod, *Int. J. Mycobacteriol.*, 2016, **5**, S161.

30 H. Gao, X. Yang, X. Tang, P. Yin and Z. Mao, *Curr. Org. Synth.*, 2019, **16**, 1032–1039.

31 V. Kali and B. Maiti, *J. Mol. Struct.*, 2024, **1299**, 137053.

32 G. Cravotto, A. Demetri, G. M. Nano, G. Palmisano, A. Penoni and S. Tagliapietra, *European J. Org. Chem.*, 2003, **2003**, 4438–4444.

33 W. Zhang, Z. Xu, Y. Tu and C. Liao, *Chinese Journal of Organic Chemistry*, 2017, **37**, 2449.

34 K. M. Khan, G. M. Maharvi, M. T. H. Khan, A. Jabbar Shaikh, S. Perveen, S. Begum and M. I. Choudhary, *Bioorg. Med. Chem.*, 2006, **14**, 344–351.

35 D. B. Ramachary and M. Kishor, *J. Org. Chem.*, 2007, **72**, 5056–5068.

36 D. Prasad, A. Preetam and M. Nath, *Comptes Rendus. Chimie*, 2012, **15**, 675–678.

37 M. Zabihzadeh, F. Shirini, H. Tajik and N. Daneshvar, *Polycycl. Aromat. Compd.*, 2021, **41**, 1972–1987.

38 Y. Zhang and Z. Shang, *Chin. J. Chem.*, 2010, **28**, 1184–1188.

39 R. Karimian, F. Piri, B. Karimi and A. Moghimi, *Croatica Chemica Acta*, 2011, 111–115.

40 Y. Ren, B. Yang and X. Liao, *RSC Adv.*, 2016, **6**, 22034–22042.

41 S. Mondal, A. M. Pandey and B. Gnanaprakasam, *React. Chem. Eng.*, 2023, **8**, 855–862.

42 D. Thakur, M. Kaur, D. S. Malhi, S. Garg, A. Sharma and H. S. Sohal, *Monatshefte für Chemie - Chemical Monthly*, 2021, **152**, 537–543.

43 M. G. Dekamin, S. Z. Peyman, Z. Karimi, S. Javanshir, M. R. Naimi-Jamal and M. Barikani, *Int. J. Biol. Macromol.*, 2016, **87**, 172–179.

44 A. Khazaee, R. Jahanshahi, S. Sobhani, J. Skibsted and J. M. Sansano, *Green Chemistry*, 2020, **22**, 4604–4616.

45 H. Alinezhad, M. Tarahomi, B. Maleki and A. Amiri, *Appl. Organomet. Chem.*, DOI:10.1002/aoc.4661.

46 N. Rostami, M. G. Dekamin, E. Valiey and H. Fanimoghadam, *Sci. Rep.*, 2022, **12**, 8642.

47 S. Gharghish, M. G. Dekamin and S. H. Banakar, *Nanoscale Adv.*, 2024, **6**, 3911–3922.

48 R. Azimi, Z. Lasemi and A. B. Hashkavayi, *Lett. Org. Chem.*, 2020, **17**, 268–280.

49 A. Yaghoubi and M. G. Dekamin, *ChemistrySelect*, 2017, **2**, 9236–9243.

50 M. A. Nasseri and S. M. Sadeghzadeh, *Journal of the Iranian Chemical Society*, 2013, **10**, 1047–1056.

51 J.-J. Yu, L.-M. Wang, J.-Q. Liu, F.-L. Guo, Y. Liu and N. Jiao, *Green Chem.*, 2010, **12**, 216–219.

52 J. Li, L. Lu and W. Su, *Tetrahedron Lett.*, 2010, **51**, 2434–2437.

53 S. Kobayashi, M. Sugiura, H. Kitagawa and W. W.-L. Lam, *Chem. Rev.*, 2002, **102**, 2227–2302.

54 K. M. Mustaque, A. Subramani, T. K. Shabeer, H. Thajudeen and V. S. J. Ahamed, *Lett. Org. Chem.*, 2018, **15**, 246–250.

55 *Susceptibility Testing of Mycobacteria,* 2011.

56 A. Campaniço, R. Moreira and F. Lopes, *Eur. J. Med. Chem.*, 2018, **150**, 525–545.

57 G. S. Shetye, S. G. Franzblau and S. Cho, *Translational Research*, 2020, **220**, 68–97.

58 L. Bunalema, G. W. Fotso, P. Waako, J. Tabuti and S. O. Yeboah, *BMC Complement. Altern. Med.*, 2017, **17**, 89.

59 M. Mpeirwe, I. M. Taremwa, P. Orikiriza, P. E. Ogwang, D. Ssesazi and J. Bazira, *Pharmacology & Pharmacy*, 2023, **14**, 33–42.

60 N. Tuyiringire, I. Taremwa Mugisha, D. Tusubira, J.-P. Munyampundu, C. Mambo Muvunyi and Y. Vander Heyden, *J. Clin. Tuberc. Other Mycobact. Dis.*, 2022, **27**, 100307.

61 D. Becerra, R. Abonia and J.-C. Castillo, *Molecules*, 2022, **27**, 4723.

62 S. Poyraz, H. A. Döndaş, C. Yamali, S. Belveren, Y. Demir, S. Aydınoglu, N. Y. Döndaş, T. Taskin-Tok, S. Taş, M. Ülger and J. M. Sansano, *J. Biomol. Struct. Dyn.*, 2024, **42**, 3441–3458.

63 J. D. Bhatt, C. J. Chudasama and K. D. Patel, *Bioorg. Med. Chem.*, 2015, **23**, 7711–7716.

64 N. Azizi, S. Dezfooli and M. M. Hashemi, *Comptes Rendus. Chimie*, 2013, **16**, 997–1001.

65 A. K. R. Ahmed, R. Gajendhiran, S. Mithra, S. A. Majeed, A. S. S. Hameed, R. Paulpandiyan, S. Maniyammai, G. T. Senthil Andavan, M. NizamMohideen and A. K. Rahiman, *J. Mater. Chem. B*, 2025, **13**, 622–641.

66 A. Hoque, M. S. Islam, M. A. Khan, S. Ghosh, Md. A. Sekh, S. Hussain and Md. A. Alam, *New Journal of Chemistry*, 2022, **46**, 16025–16034.

67 M. Mpeirwe, I. M. Taremwa, P. Orikiriza, P. E. Ogwang, D. Ssesazi and J. Bazira, *Pharmacology & Pharmacy*, 2023, **14**, 33–42.

68 A. Cohen, V. D. Mathiasen, T. Schön and C. Wejse, *European Respiratory Journal*, 2019, **54**, 1900655.

Supplementary Files

This is a list of supplementary files associated with this preprint. Click to download.

- DXSUPPLIMENTARY.docx